Supplementary Materials

Influence of the thermal processing and doping of $LaMnO_3$ and $La_{0.8}A_{0.2}MnO_3$ (A=Ca, Sr, Ba) perovskites prepared by auto-combustion for removal of VOCs

Natasha Di Benedetto[1], Carolina De los Santos[2,*], María del Pilar Yeste[3], Jonder Morais[4], Maria do Carmo Martins Alves[5], Alejandro Amaya[2], Leopoldo Suescun[1,*], José Manuel Gatica[3], Hilario Vidal[3] and Jorge Castiglioni[2]

[1] Laboratorio de Cristalografía, Química del Estado Sólido y Materiales/DETEMA/Facultad de Química/Universidad de la República, Av. Gral. Flores 2124, Montevideo 11800, Uruguay

[2] Laboratorio de Fisicoquímica de Superficies/Área Fisicoquímica/DETEMA/Facultad de Química/Universidad de la República, Av. Gral. Flores 2124, Montevideo 11800, Uruguay

[3] Departamento C.M. I.M. y Química Inorgánica, Universidad de Cádiz, Puerto Real 11510, Spain

[4] Laboratório de Espectroscopia de Elétrons (LEe-), Instituto de Física – Universidade Federal do Rio Grande do Sul, 91501-970 Porto Alegre, RS, Brazil

[5] Instituto de Química - Universidade Federal do Rio Grande do Sul, 91501-970, Porto Alegre, RS, Brazil

* Correspondence: leopoldo@fq.edu.uy (L.S.); cdlsantos@fq.edu.uy (C.DlS.)

Table S1. ICP-AES spectroscopic results obtained for LM, LCM, LSM and LBM samples

Sample	% La (atomic)	% Mn (atomic)	% Sr (atomic)	% Ca (atomic)	% Ba (atomic)
LM	50.2 ± 1.8	49.8 ± 2.2	-	-	-
LSM	41.5 ± 1.7	50.2 ± 2.8	9.3 ± 0.4	-	-
LCM	40.9 ± 1.9	50.6 ± 3.3	-	8.4 ± 0.9	-
LBM	40.7 ± 1.7	50.1 ± 2.3	-	-	9.1 ± 0.1

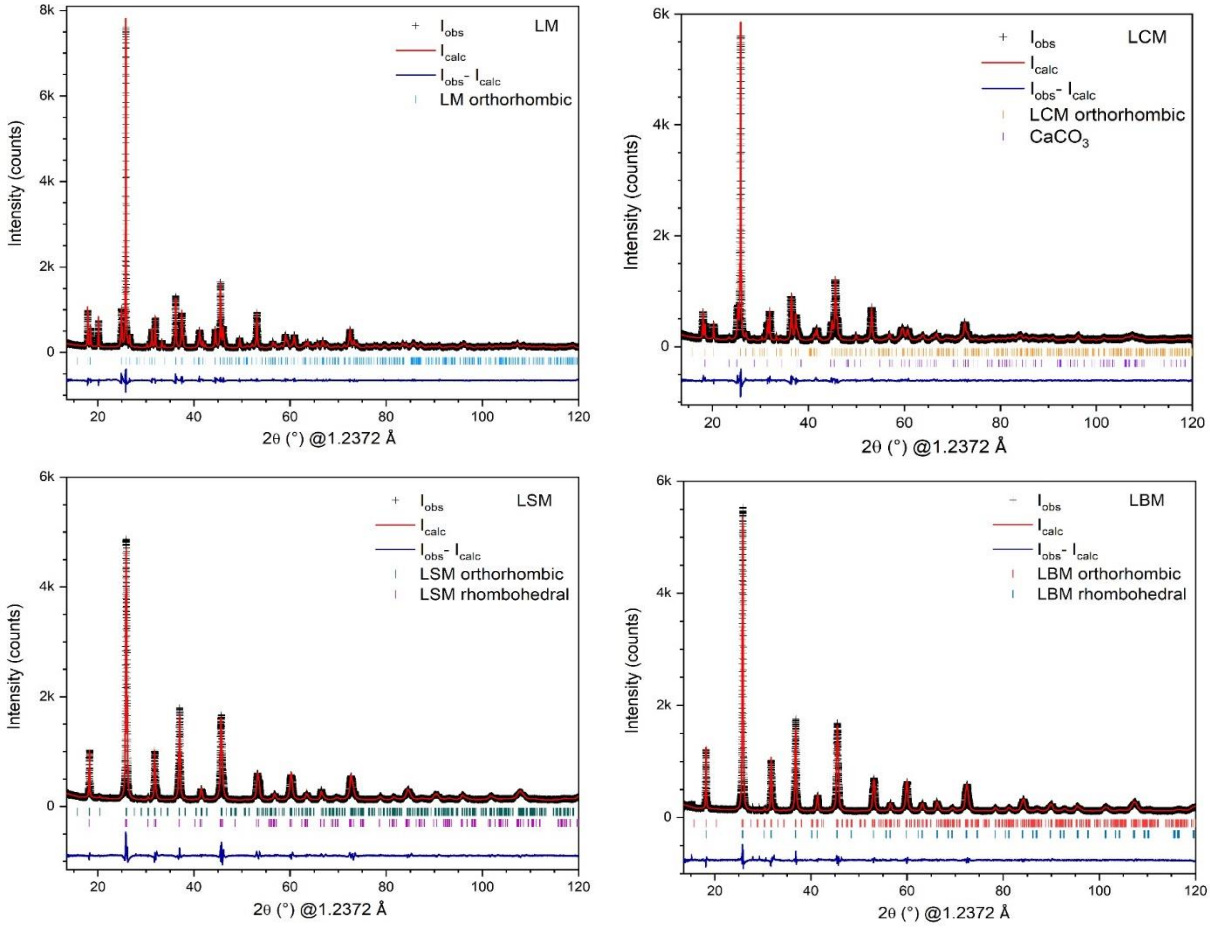

Figure S1. Rietveld fit of synchrotron XRD patterns of the as-prepared samples confirming the presence of pure manganites with perovskite structure (except for LCM that exhibits a 4.7% weight of $CaCO_3$ impurity). The LSM and LBM samples are mixtures of orthorhombic Pbnm and rhombohedral Rc perovskite phases.

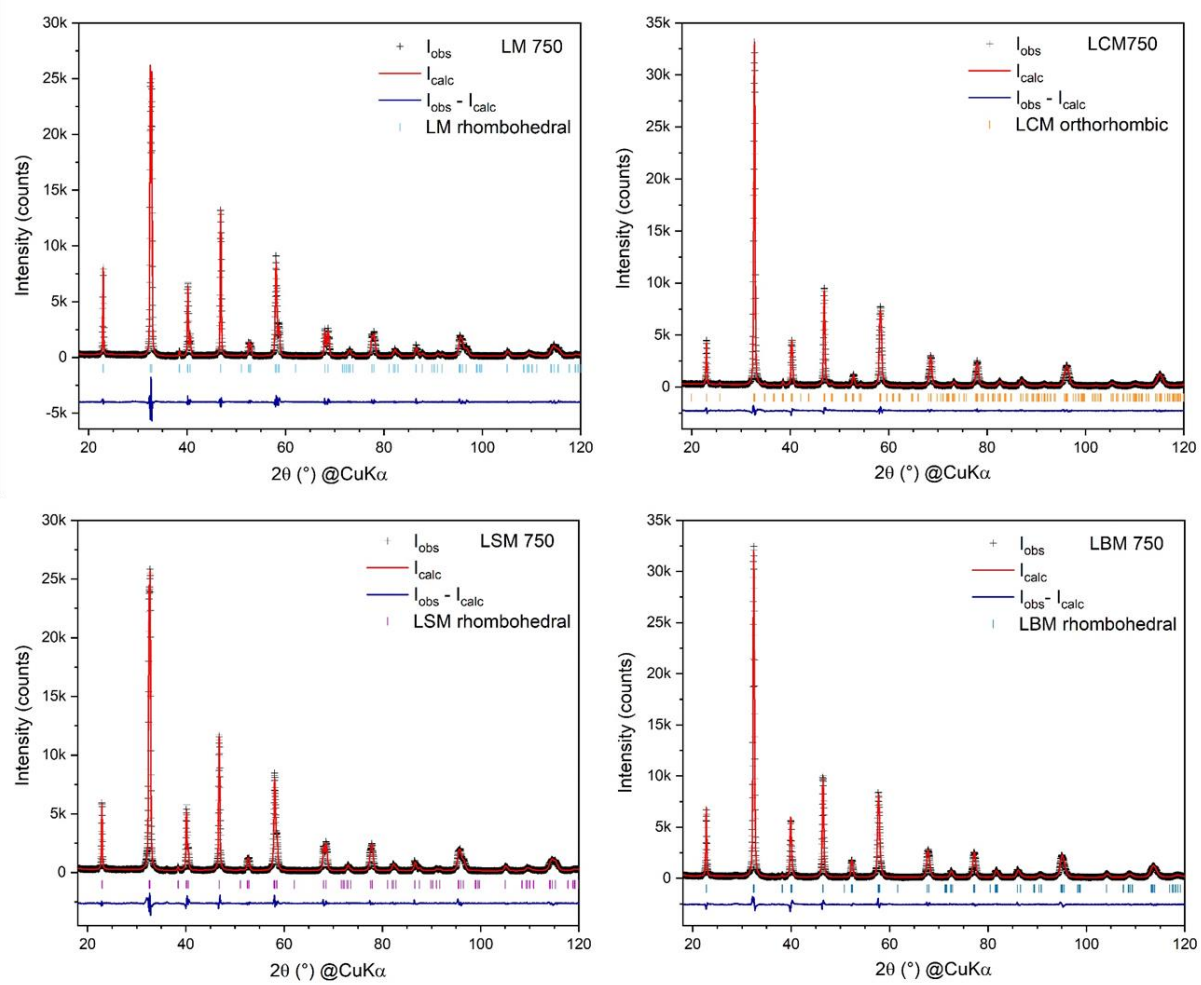

Figure S2. Rietveld fit of conventional XRD diffractograms of the calcined samples.

Table S2. Final parameters for the as-prepared samples XRD data obtained through Rietveld fit.

Sample	S.G.	weight %	a (Å)	b (Å)	c (Å)	Rw (%)
LM	Pbnm	100	5.53931	5.73236	7.70336	5.677
LM750	$R\bar{3}c$	100	5.51481	-	13.34143	7.791
LCM	Pbnm	95.3	5.53691	5.65096	7.72597	5.296
LCM750	Pbnm	100	5.46882	5.50379	7.74017	7.119
LSM	Pbnm	58.2	5.54016	5.51013	7.78367	3.733
	$R\bar{3}c$	41.8	5.53273	-	13.38227	
LSM750	$R\bar{3}c$	100	5.51039	-	13.3657	7.631
LBM	Pbnm	70.7	5.52219	5.56188	7.8192	4.424
	$R\bar{3}c$	29.3	5.54177	-	13.57041	
LBM750	$R\bar{3}c$	100	5.53637	-	13.48379	7.764

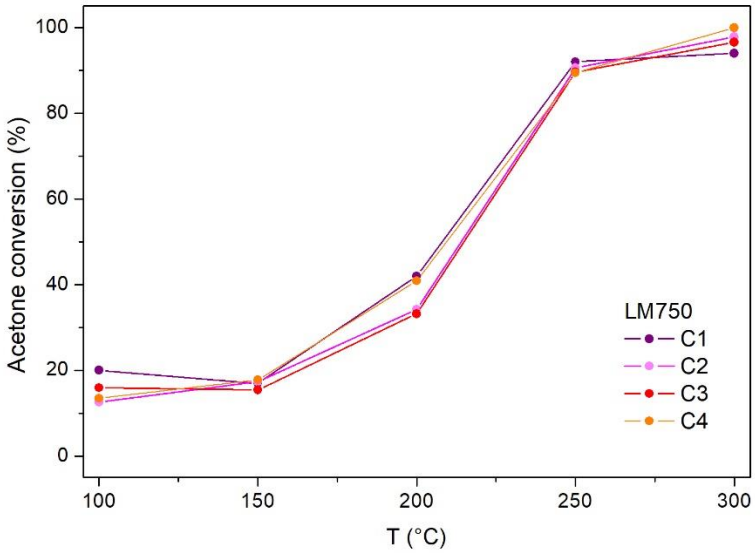

Figure S3. Acetone conversion of LM750 over four consecutive cycles showing no sign of catalyst deactivation.

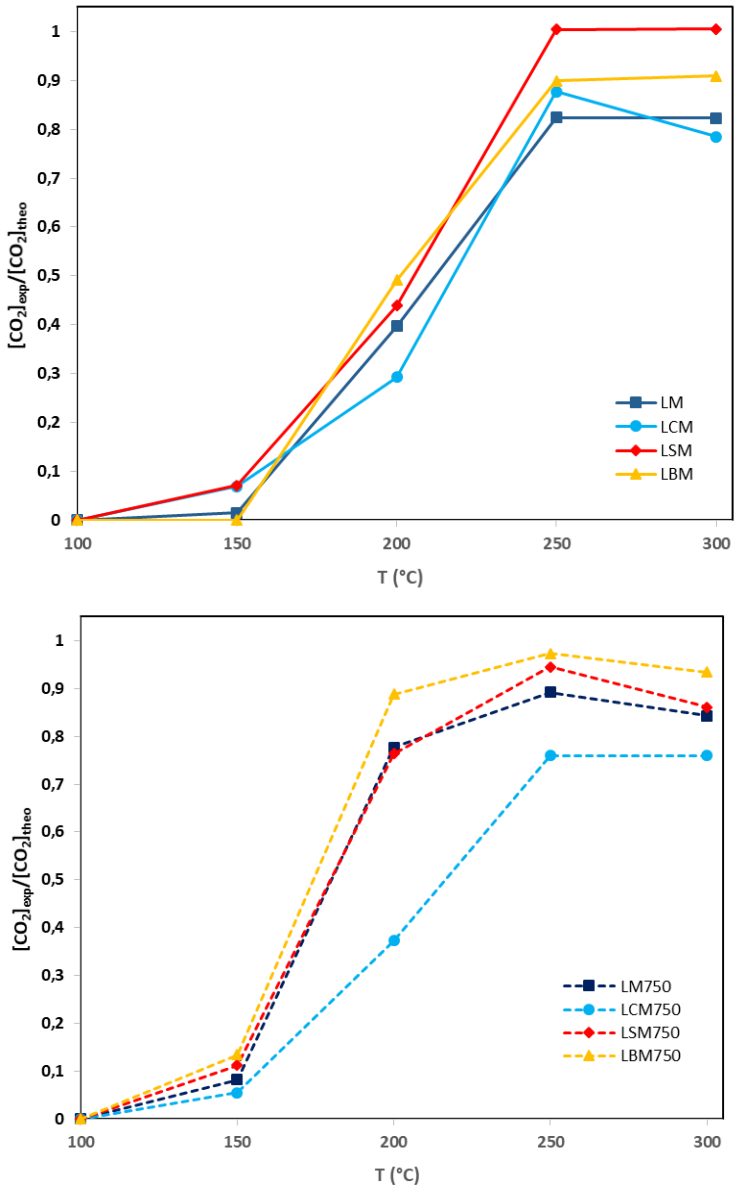

Figure S4. $[CO_2]_{experimental}/[CO_2]_{theoretical}$ ratio vs temperature curves for the as-prepared manganites and the calcined samples.

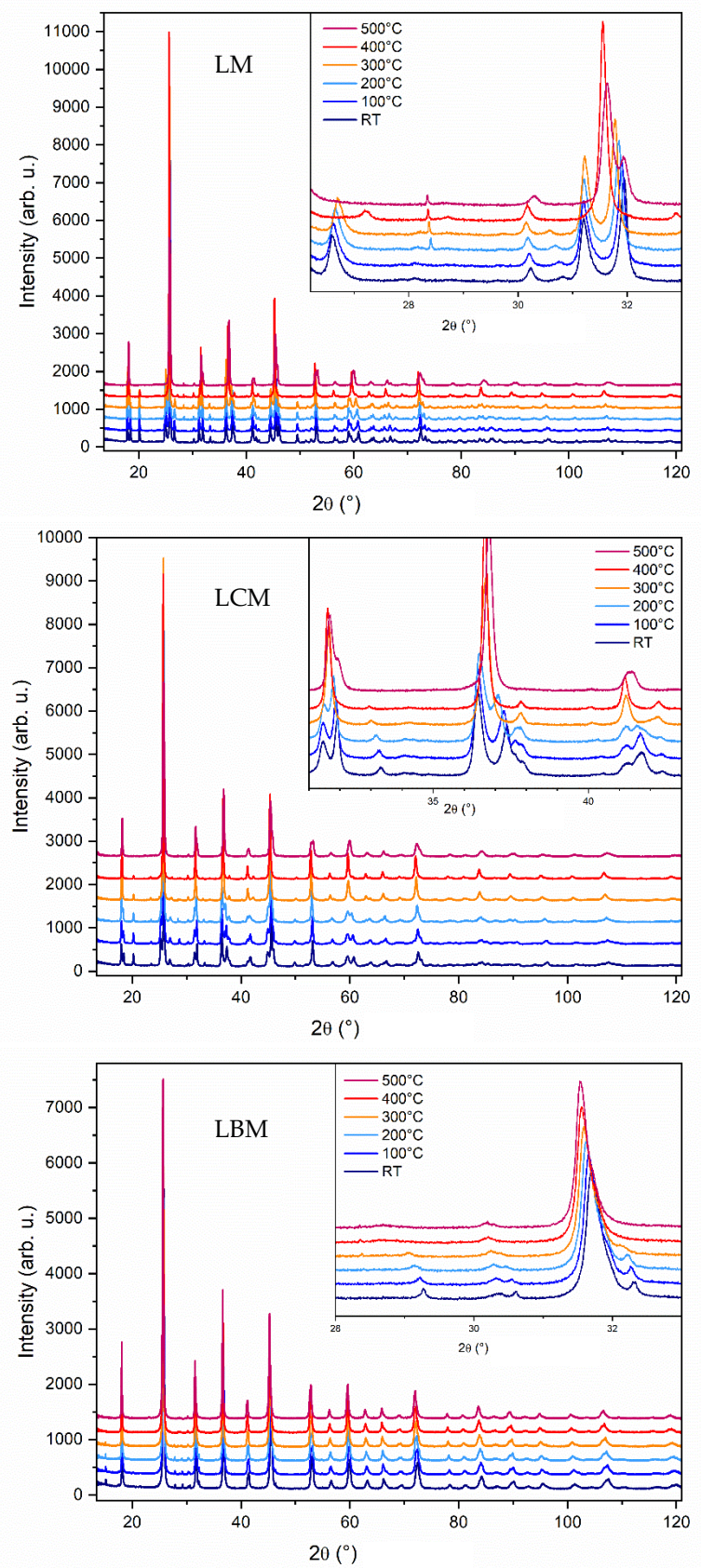
LM
500°C
400°C
300°C
200°C
100°C
RT
Intensity (arb. u.)
2θ (°)
LCM
500°C
400°C
300°C
200°C
100°C
RT
Intensity (arb. u.)
2θ (°)
LBM
500°C
400°C
300°C
200°C
100°C
RT
Intensity (arb. u.)
2θ (°)

Figure S5. Synchrotron XRD patterns of the indicated as-prepared samples heated from RT to 500 °C in air. The insets show in more detail the appearance/disappearance of some peaks during the heating process.

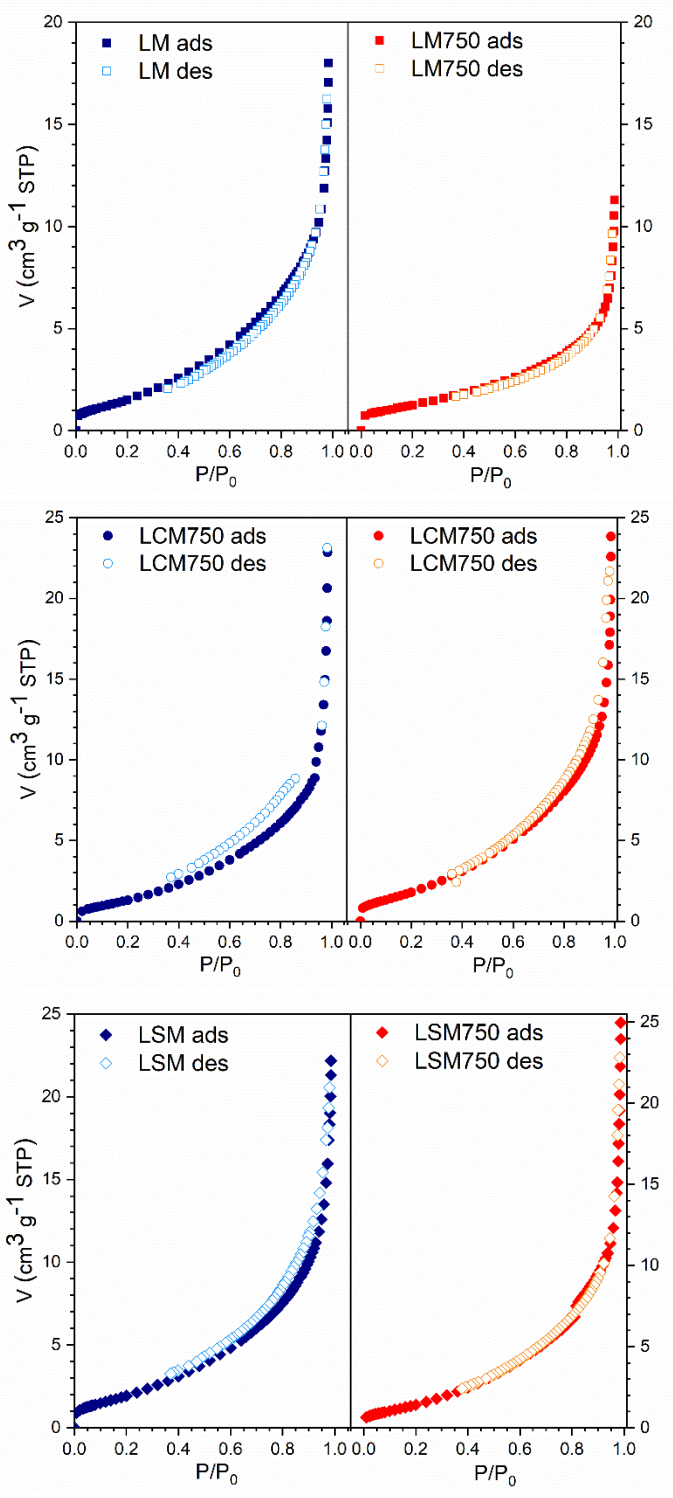

Figure S6. N_2 physisorption isotherms for the indicated as-prepared and calcined samples.

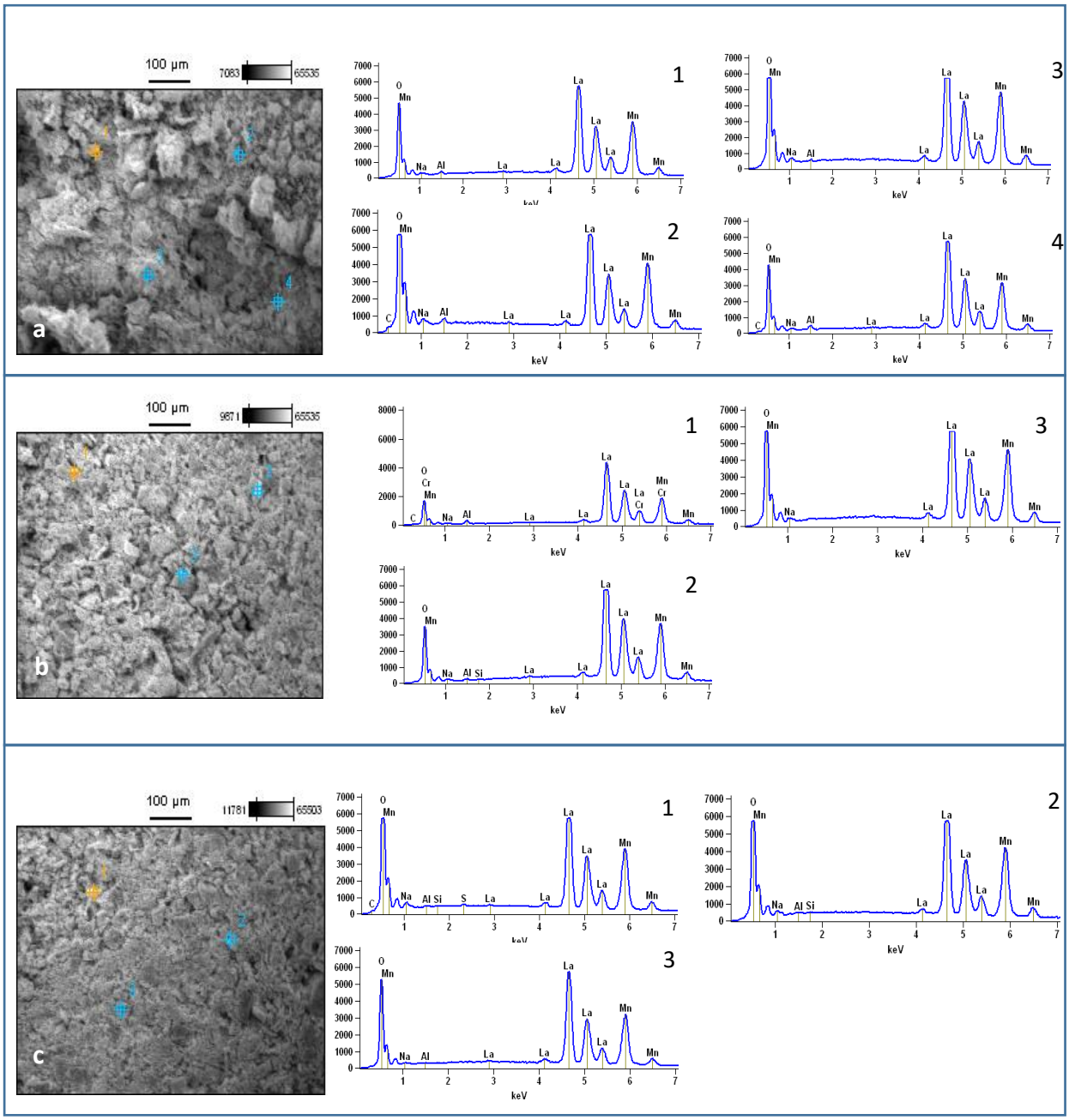

Figure S7. SEM images with EDS analysis corresponding to different zones of LM: (a) zone 1, (b) zone 2 and (c) zone 3.

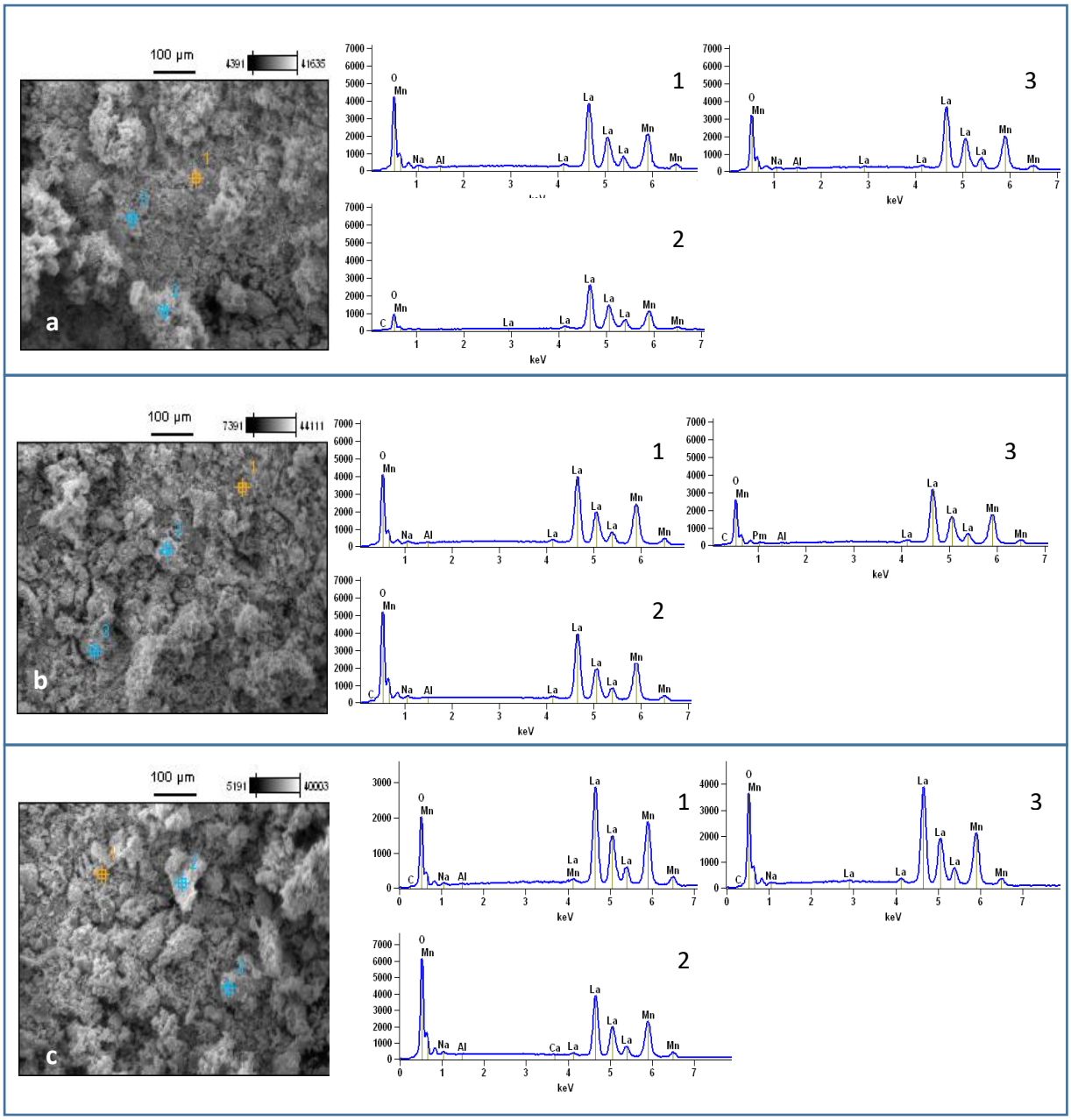

Figure S8. SEM images with EDS analysis corresponding to different zones of LM750: (a) zone 1, (b) zone 2 and (c) zone 3.

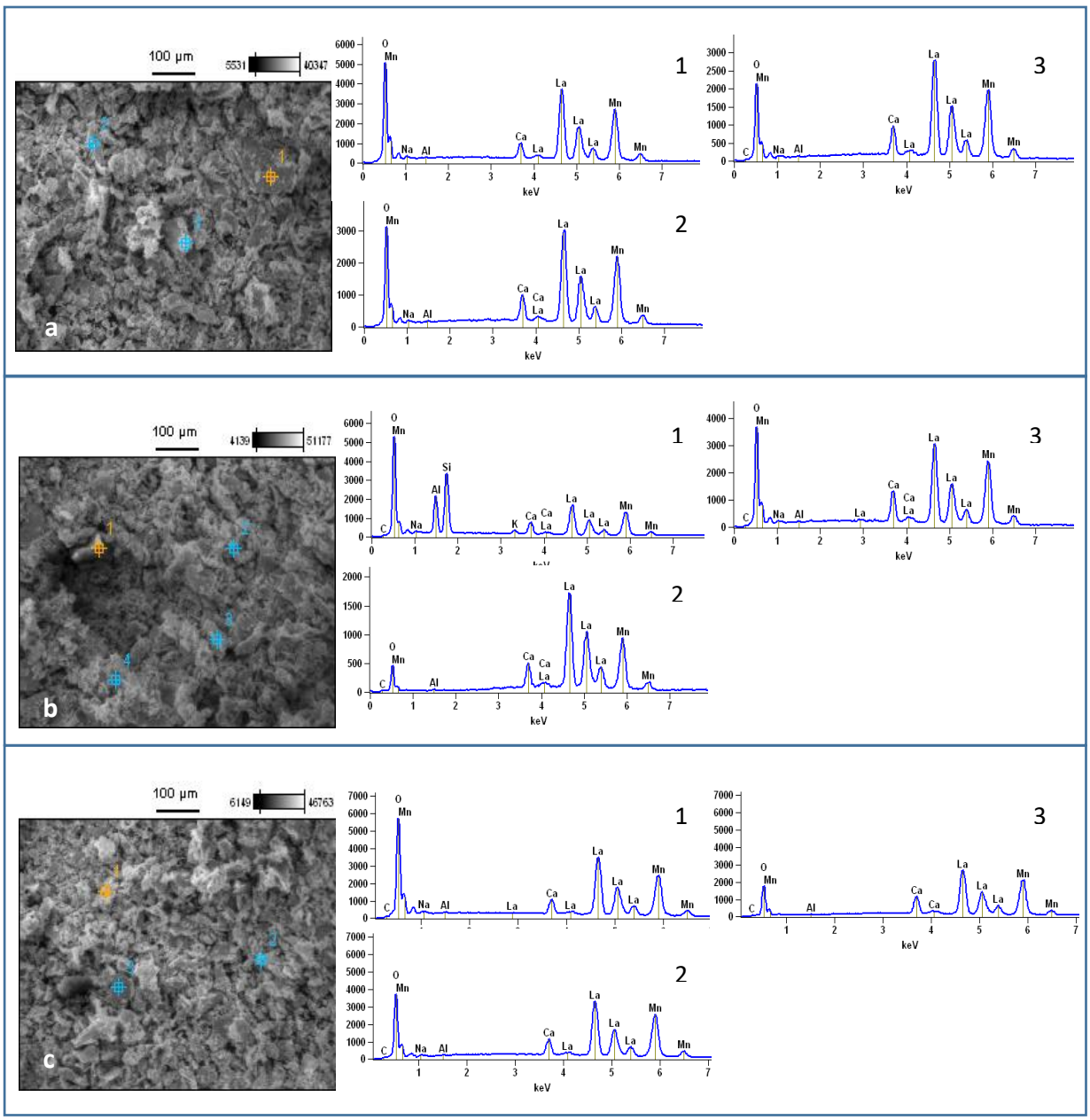

Figure S9. SEM images with EDS analysis corresponding to different zones of LCM: (a) zone 1, (b) zone 2 and (c) zone 3.

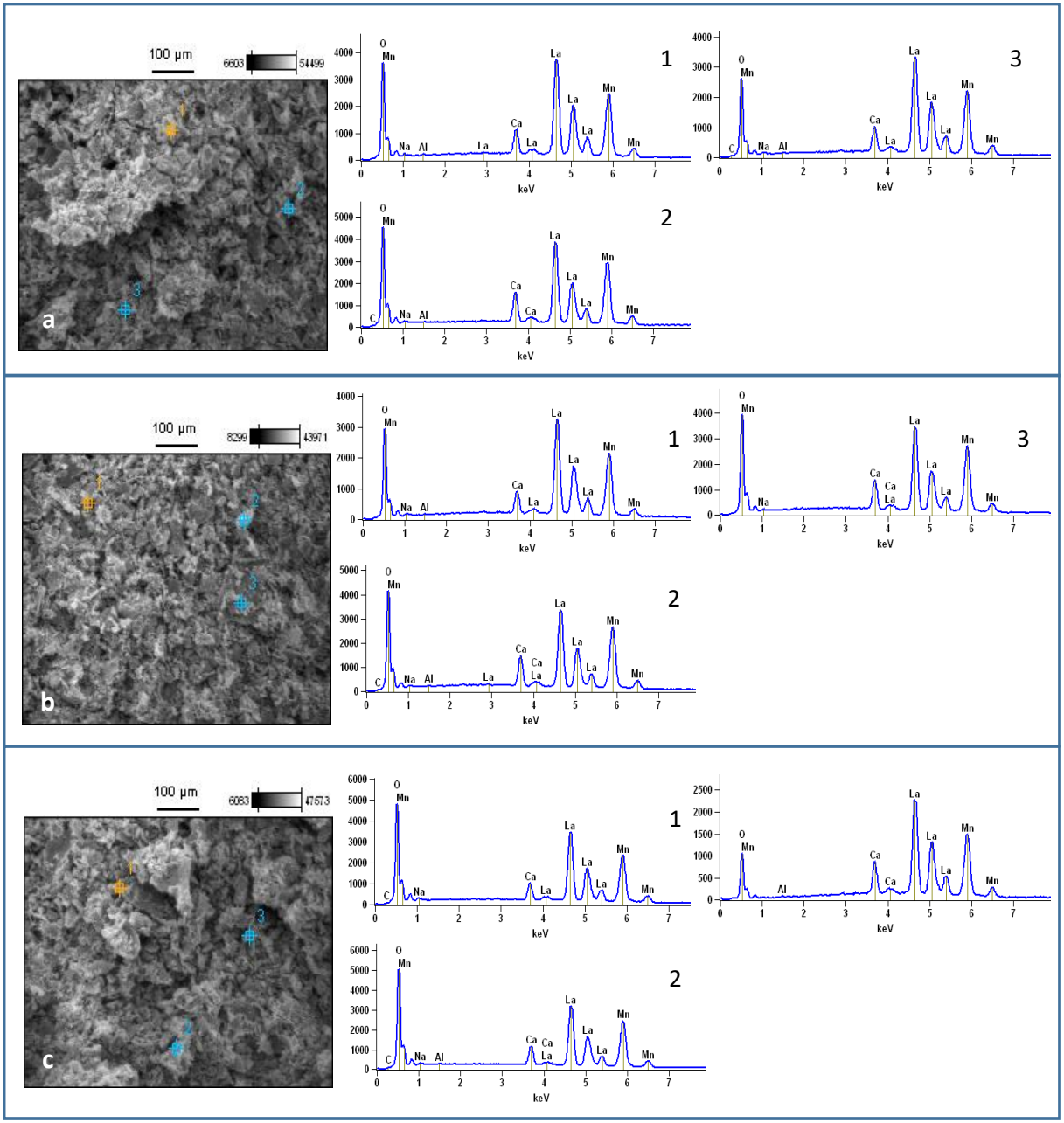

Figure S10. SEM images with EDS analysis corresponding to different zones of LCM750: (a) zone 1, (b) zone 2 and (c) zone 3.

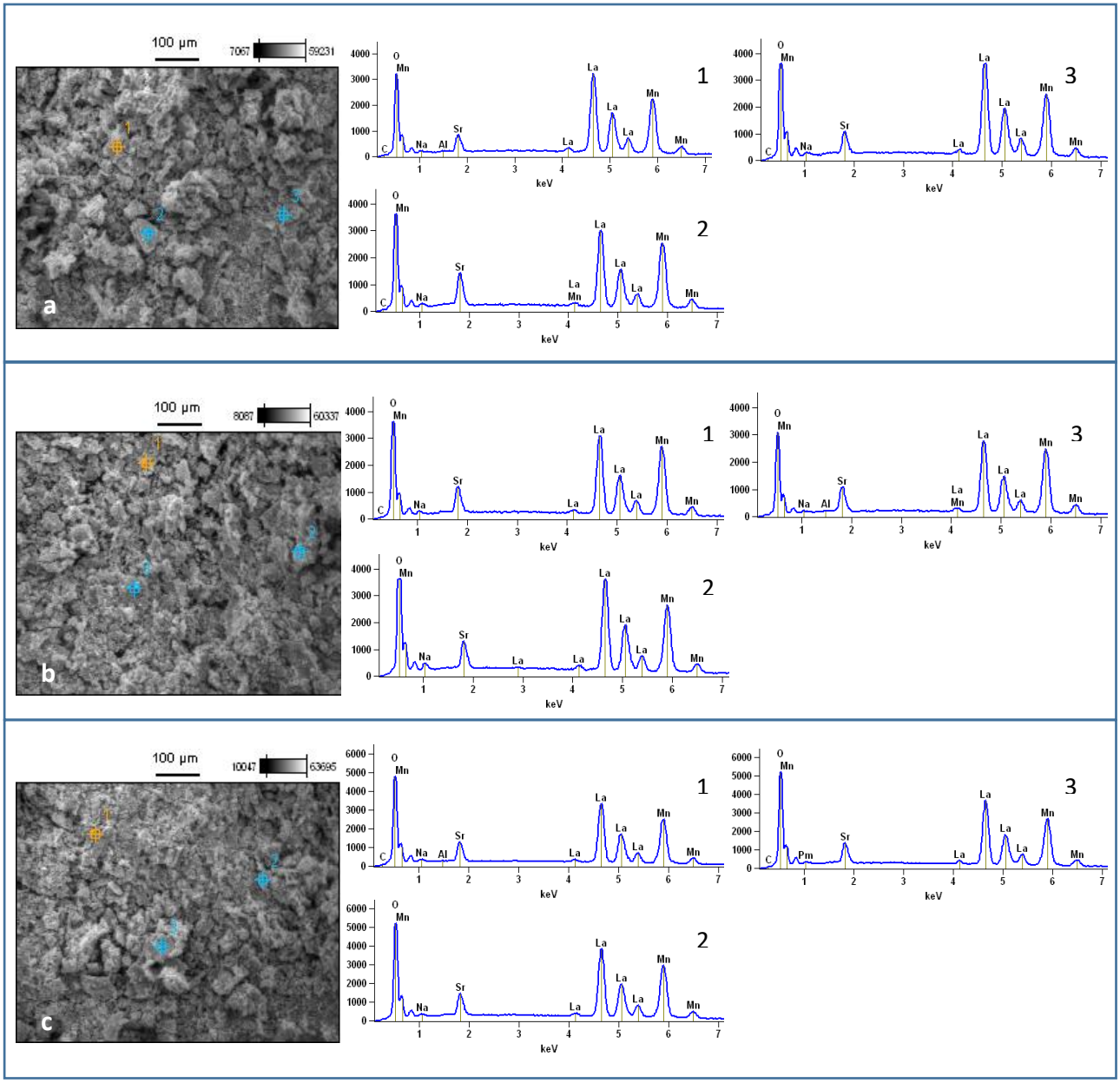

Figure S11. SEM images with EDS analysis corresponding to different zones of LSM: (a) zone 1, (b) zone 2 and (c) zone 3.

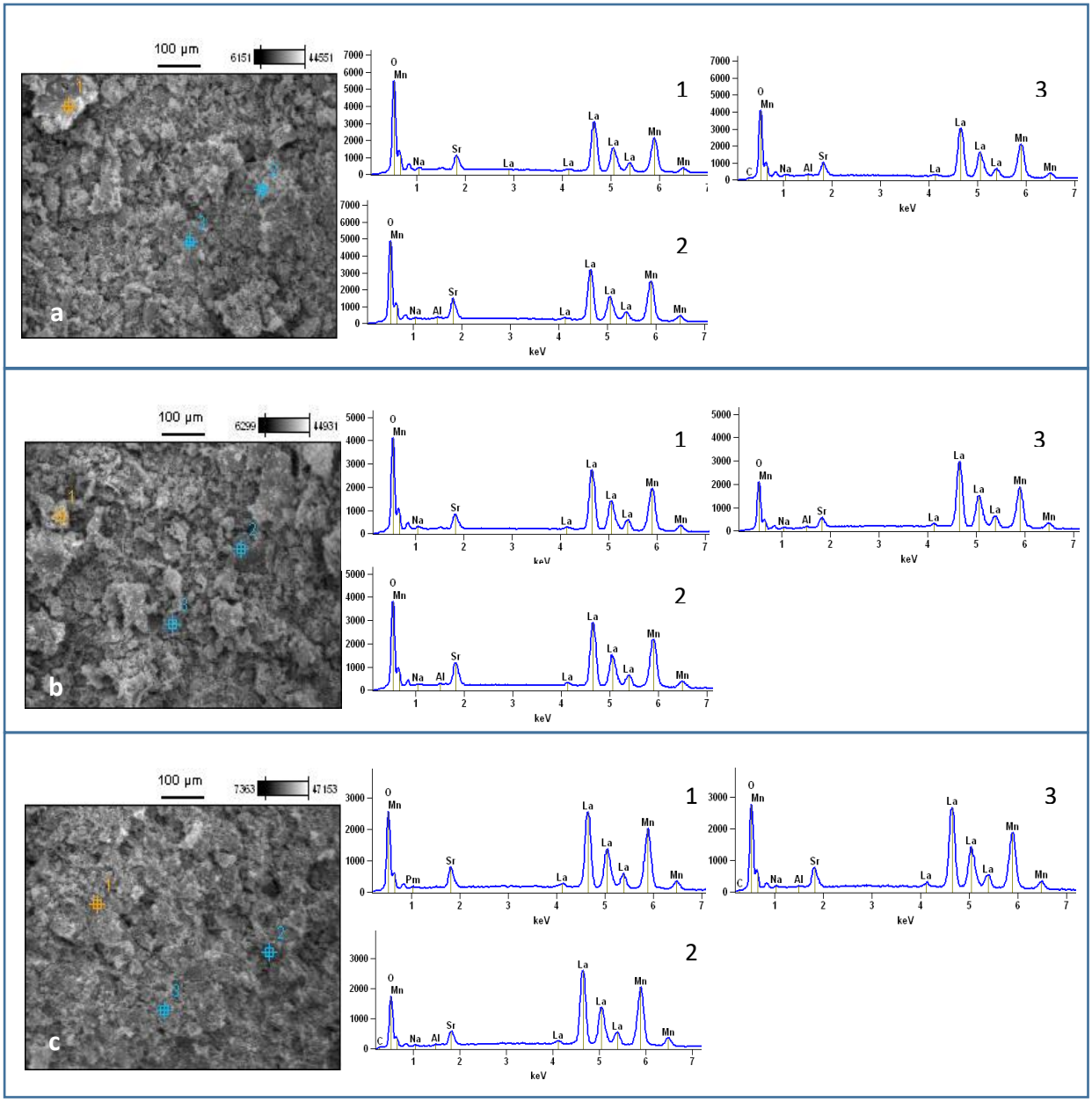

Figure S12. SEM images with EDS analysis corresponding to different zones of LSM750: (a) zone 1, (b) zone 2 and (c) zone 3.

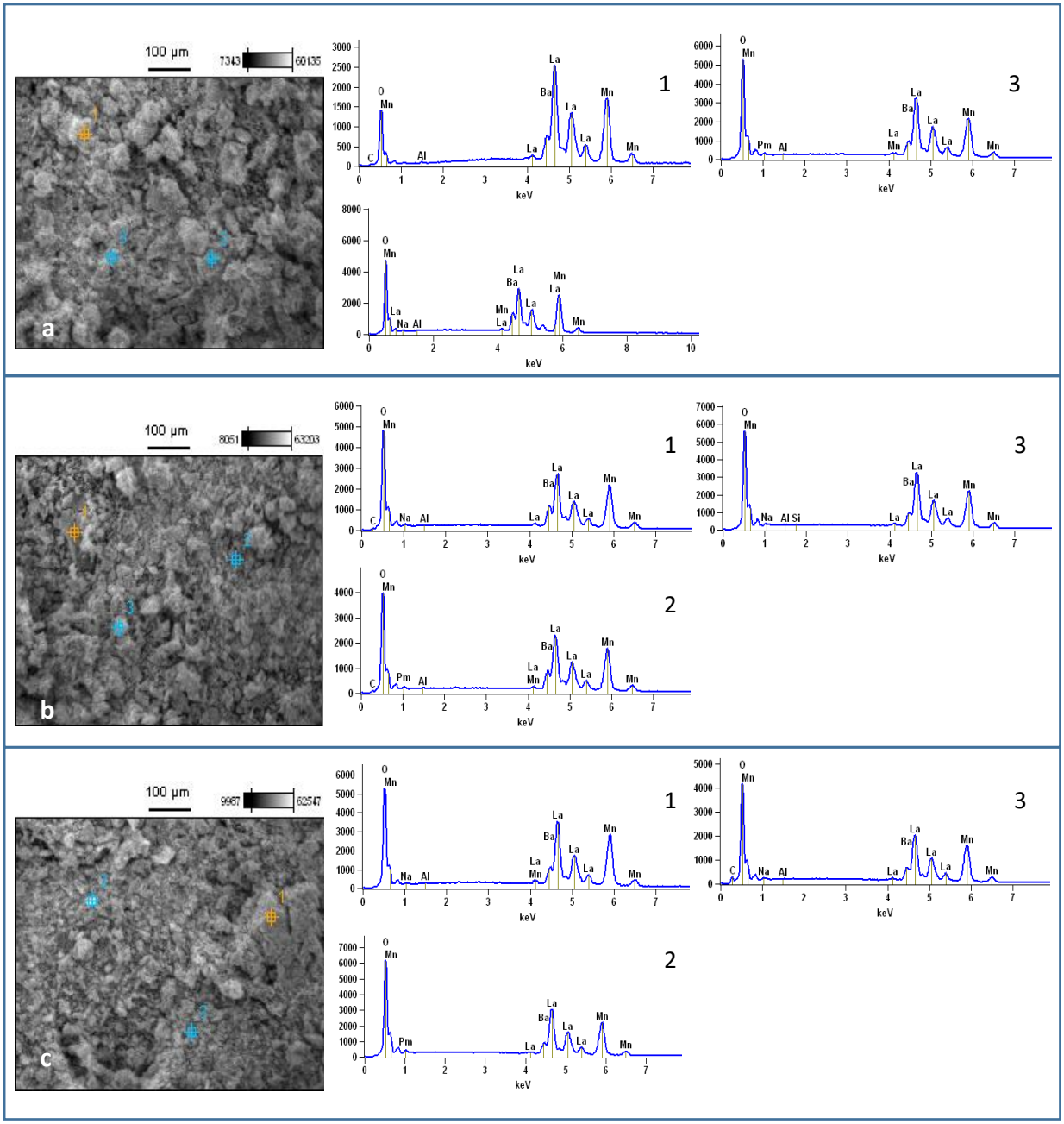

Figure S13. SEM images with EDS analysis corresponding to different zones of LBM: (a) zone 1, (b) zone 2 and (c) zone 3.

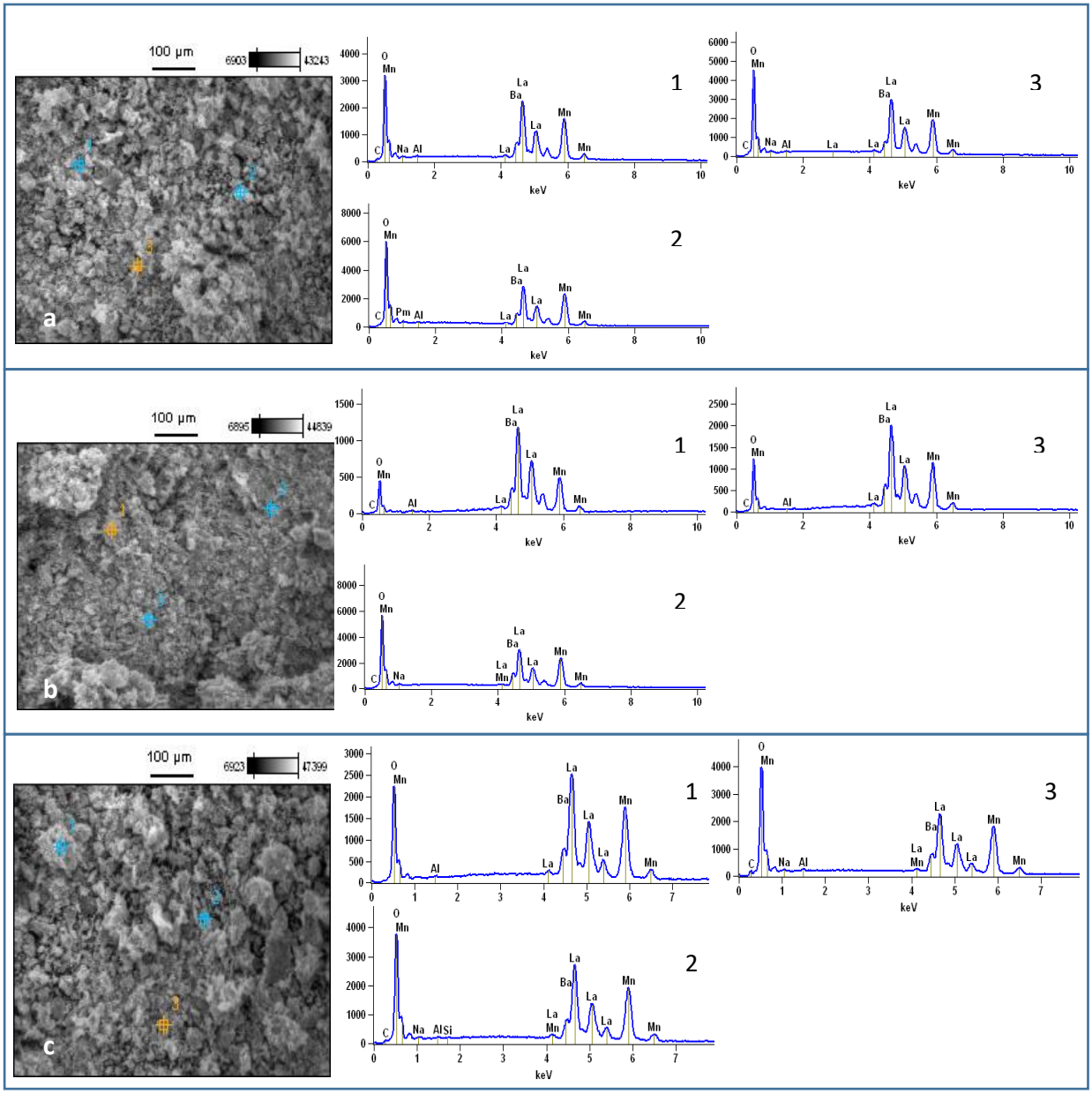

Figure S14. SEM images with EDS analysis corresponding to different zones of LBM750: (a) zone 1, (b) zone 2 and (c) zone 3.

Table S3. Atom % obtained by EDS corresponding to the points indicated in the different zones of the SEM images for the LM, LM750, LCM and LCM 750 samples.

Sample	Zone	Atom %		
		O	**Mn**	**La**
LM	1	53.3	21.1	23.2
		51.5	19.8	24.9
		38.0	22.5	33.8
		67.1	13.4	14.1
	2	60.4	18.4	20.1
		44.3	23.6	30.4
		63.2	17.0	18.1
	3	63.3	15.6	16.8
		63.5	17.1	17.6
		59.0	18.5	21.3
LM750	1	49.2	24.7	23.0
		68.0	14.6	15.1
		58.1	19.0	21.2
	2	61.5	17.1	19.3
		37.9	25.0	36.7
		58.3	18.4	21.3
	3	59.6	19.5	19.0
		65.7	15.4	16.5
		55.2	20.3	23.2
LCM	1	65.0	16.4	14.3
		59.1	19.2	16.2
		53.2	21.3	19.2
	2	27.0	27.9	35.3
		61.2	18.2	14.4
		55.3	20.1	19.2
	3	69.2	14.0	12.5
		60.0	19.3	15.7
		48.6	24.4	19.8
LCM750	1	57.6	18.6	18.2
		60.3	18.3	15.1
		52.7	20.9	20.3
	2	57.5	19.2	18.2
		62.0	17.4	14.1
		61.5	18.3	14.7
	3	65.4	15.9	14.2
		67.5	14.5	12.2

	40.6	26.2	25.7

Table S4. Atom % obtained by EDS corresponding to the points indicated in the different zones of the SEM images for the LSM, LSM750, LBM and LBM 750 samples.

Sample	Zone	Atom %		
		O	Mn	La
LSM	1	58.2	18.2	17.0
		63.8	16.8	12.6
		62.5	16.1	15.6
	2	62.6	18.0	13.6
		66.9	14.6	12.9
		59.9	20.0	14.0
	3	67.0	14.8	12.6
		66.0	16.0	13.1
		67.8	15.2	12.9
LSM750	1	71.2	12.7	11.8
		67.9	14.8	11.4
		65.3	14.9	13.9
	2	67.3	15.0	13.3
		64.6	16.2	13.0
		53.1	20.8	21.4
	3	59.3	19.5	16.8
		48.4	25.1	20.4
		58.7	18.2	16.2
LBM	1	42.4	26.9	23.7
		63.5	17.6	12.7
		67.8	15.0	13.9
	2	66.0	15.2	12.0
		66.1	15.6	12.7
		67.6	14.2	13.4
	3	64.2	17.5	13.3
		71.0	14.2	12.1
		59.3	11.6	9.0
LBM750	1	61.9	16.6	14.7
		69.4	14.3	11.0
		65.0	15.3	14.6
	2	35.1	22.3	33.6
		67.6	15.3	12.2
		45.1	22.1	25.0
	3	53.3	21.6	19.8
		61.7	16.8	14.6

	61.1	14.3	11.0

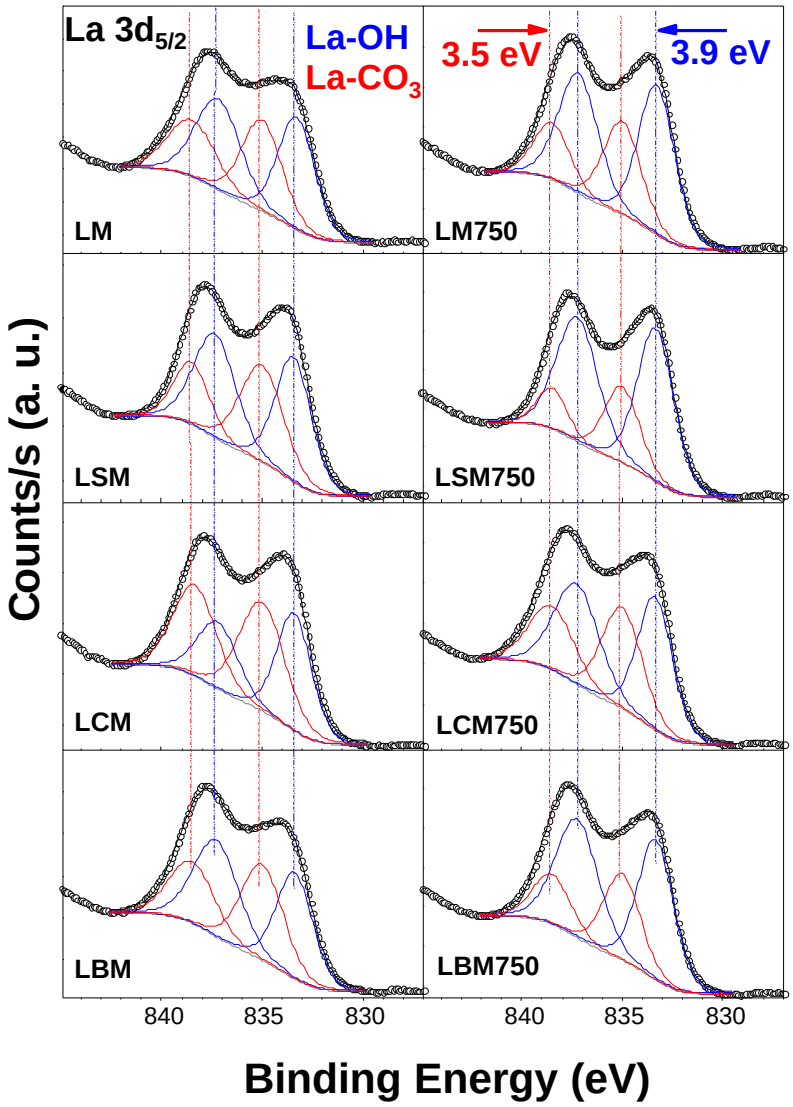

Figure S15. La $3d_{5/2}$ XPS spectra (dots) for all samples before and after the thermal treatments fitted with two chemical components, named La-OH (blue lines) and La-CO_3 (red lines), which present 3.9 and 3.5 eV splitting, respectively.

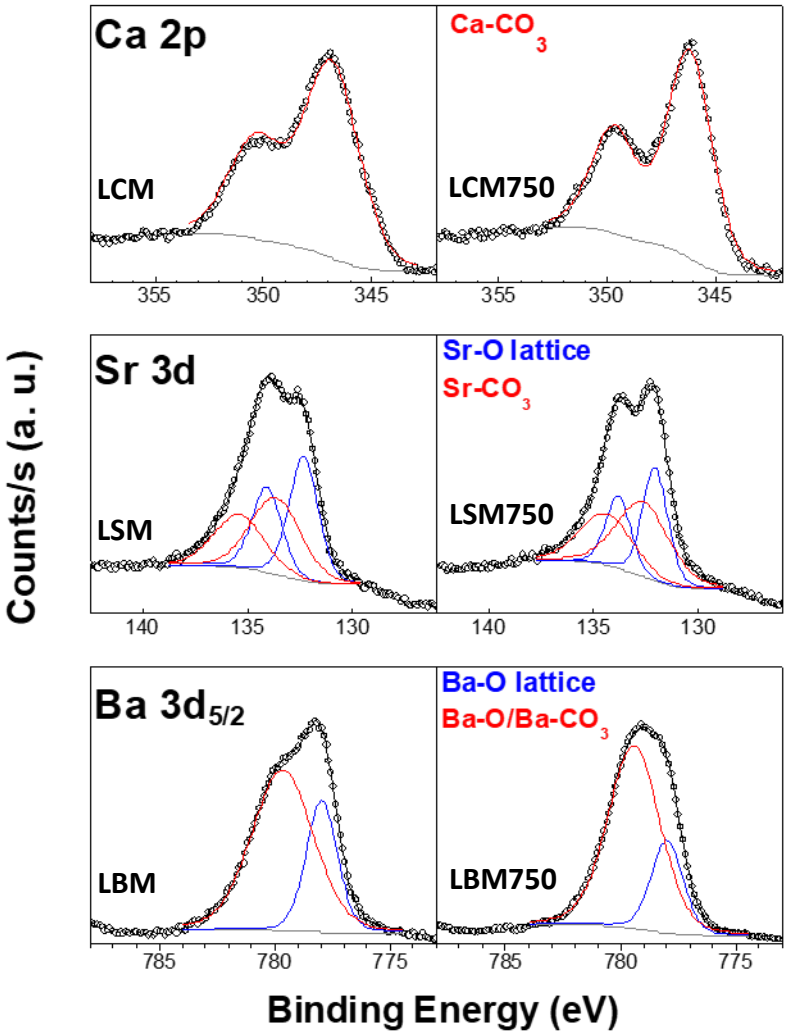

Figure S16. Ca 2p, Sr 3d, and Ba $3d_{5/2}$ high-resolution XPS spectra (dots) acquired before and after the thermal treatments. Also shown are the corresponding chemical components indicated in the figure legends (blue and red lines).

Interpretation of XPS results

Figure S15 shows the high resolution La $3d_{5/2}$ XPS spectra of the as-prepared and calcined samples. The La 3*d* signal presents well separated spin-orbit components ($3d_{3/2}$ and $3d_{5/2}$) where each component can be fitted considering further multiplet splitting [1] with well-known energy separation. Therefore, the La $3d_{5/2}$ region fit requires two pairs of peaks corresponding to two chemical components, named La-OH (hydroxide) and La-CO_3 (carbonate), each presenting 3.9 and 3.5 eV splitting, respectively. This is a more accurate approach to ascertain the lanthanum chemical components rather than by determining the $3d_{5/2}$ peak position, since the later have very close binding energy values for distinct La chemical states (for instance, La_2O_3, $La(OH)_3$ or $La_2(CO_3)_3$). Based on the fit it was possible to conclude that La atoms in a mixed oxide state, i.e. La_2O_3, are not present, which would correspond to a component presenting a 4.6 eV multiplet splitting. [2] The presence of surface hydroxide and carbonate is not a surprise since La compounds may hydrolyze and easily form carbonates by reacting with CO_2

at room temperature. The XPS signals emitted by the A metals in $La_{0.8}A_{0.2}MnO_3$ samples are shown in Figure S16. The Ca 2*p*, Sr 3*d*, and Ba $3d_{5/2}$ peaks were fitted considering different chemical components for each case [3]. For the LCM and LCM750 samples, the Ca 2*p* spectrum clearly presents only one chemical component assigned to $CaCO_3$, which was also fitted with two peaks (Ca $2p_{1/2}$ and Ca $2p_{3/2}$) separated by the spin orbit splitting of 3.5 eV. In the case of LSM and LSM750 samples, two chemical components were required in order to fit the Sr 3*d*, corresponding to Sr-O bonds in the structure and Sr-CO_3 bonds (carbonate). Each component consisted of two peaks accounting for the spin orbit splitting (Sr $3d_{3/2}$ and Sr $3d_{5/2}$). Regarding the LBM and LBM750 samples, the Ba $3d_{5/2}$ peak fitting demanded the use of two chemical states, one at lower binding energy that is related to Ba-O bonds in the structure, and another wider component that can be assigned to either Ba-O species (non-bulk) or Ba-CO_3 bonds (carbonate). Based solely on the XPS results shown above, it is most likely this wider component is mainly a result of surface carbonates.

References

1. Shirley, D.A. High-Resolution X-Ray Photoemission Spectrum of the Valence Bands of Gold. *Phys. Rev. B* **1972**, *5(12)*, 4709-4714.

2. Sunding, M.F.; Hadidi, K.; Diplas, S.; Lovvik, O.M.; Norby, T.E.; Gunnaes, A.E. XPS characterization of in situ treated lanthanum oxide and hydroxide using tailored charge referencing and peak fitting procedures. *J. Electron Spectrosc. Related Phenom.* **2011**, *184*, 399-409.

3. Li, J.P.H.; Zhou, X.; Pang, Y.; Zhu, L.; Vovk, E.I.; Cong, L.; van Bavel, A.P.; Li, S.; Yang, Y. Understanding of binding energy calibration in XPS of lanthanum oxide by in situ treatment. *Phys. Chem. Chem. Phys.* **2019**, *21*, 22351.